ASSOCIAÇÃO BRASILEIRA DE ENERGIA NUCLEAR – ABEN
2019 International Nuclear Atlantic Conference - INAC 2019
Santos, SP, Brazil, October 21-25, 2019

Agência Brasileira do ISBN
ISBN 978-85-99141-08-3
9 788599 141083

CRYSTALLOGRAPHIC TEXTURE OF HOT ROLLED URANIUM-MOLYBDENUM ALLOYS

Guilherme F. Nielsen[1,2], Nathanael Wagner S. Morais[2], Selma Luiza Silva[1] and Nelson B. de Lima[2]

[1] Departamento de Materiais Nucleares – Centro Industrial Nuclear de Aramar
Rodovia Sorocaba-Iperó Km 12,5
18560-000, Iperó, SP, Brazil
guilherme.nielsen@marinha.mil.br

[2] Instituto de Pesquisas Energéticas e Nucleares (IPEN / CNEN - SP)
Av. Professor Lineu Prestes 2242
05508-000 São Paulo, SP, Brazil
nblima@ipen.br

ABSTRACT

The uranium molybdenum (U-Mo) alloys have potential to be used as low enriched uranium nuclear fuel in research, test and power nuclear reactors. U-Mo alloy with composition between 7 and 10 wt% molybdenum shows excellent body centered cubic phase (γ phase) stabilization and presents a good nuclear fuel testing performance. Hot rolling is commonly utilized to produce parallel fuel plate where it promotes bonding the cladding and the fuel alloy. The mechanical deformation generates crystallographic preferential orientation, the texture, which influences the material properties. This work studied the texture evolution in hot rolled U-Mo alloys. The U7.4Mo and U9.5Mo alloys were melted in a vacuum induction furnace, homogenized at 1000°C for 5 h and then hot rolled at 650°C in three height reductions: 50, 65 and 80%. The as-cast and processed alloys microstructures were characterized by optical and electronic microscopies. The crystalline phases and the texture were evaluated by X-ray diffraction (XRD). The as-cast, homogenized and deformed alloys have γ phase. It was found microstructural differences between the U7.4Mo and U9.5Mo alloys. The homogenized treatment showed effective for microsegregation reduction and were not observed substantial grain size increasing. The deformed uranium molybdenum alloys presented strong γ fiber texture (111) <*uvw*> and moderated α-fiber texture (*hkl*) <110>.

1. INTRODUCTION

The Reduced Enrichment Program for Research and Test Reactors (RERTR) was initiated in 1978 to develop technology to convert nuclear reactors to operate with low uranium enrichment nuclear fuels [1], [2]. This program limited established nuclear fuels production enrichment up to 20% by weight of the fissile isotope ^{235}U, called Low Enriched Uranium (LEU).

Higher fuel load or the production of nuclear fuels with high concentration of fissile material are proposed solutions to feasible the use of LEU [3]–[5].

Monolithic fuels are employed to increase the density of fissile material in nuclear fuels. These fuels are usually produced in the form of plates where their core is the fissile material and its cladding by zirconium or stainless steel. These fuels have high thermal conductivity

and intermediate melting point. This high content of fissile material in thick plates, however, may be undesirable because it causes excessive swelling [1], [6].

Pure uranium has orthorhombic uranium crystal system (α-U) at room temperature. This crystalline phase has some disadvantages such as high chemical reactivity (low oxidation resistance and high pyrophoricity), anisotropy of properties and swelling by irradiation [6]. To get better nuclear fuel the metastable body centered cubic (γ phase) is desirable to achieve. To stabilize the gamma phase alloying elements are added [7]. The uranium-molybdenum alloy is most commonly used monolithic fuels. This alloy from 7wt% of molybdenum stabilizes γ-uranium [1], [8]. U10Mo was selected as a candidate with the best performance characteristics. These performance factors include minimum fuel swelling and also phase stability [9].

For the production of fuel plates, the rolling technique is the most employed [1], [10], [11]. For bonding the fuel core and the cladding, hot rolling process is normally used. Deformation processes modify the material microstructure and generate the preferential crystallographic orientation, the texture.

The understanding of the evolution of the microstructure and the mechanical properties during hot rolling is therefore essential to predict the behavior of the alloy under operational conditions and their damage by irradiation [10].

This work will evaluate the crystallographic behavior under different conditions of deformation by hot rolling.

2. EXPERIMENTAL

The alloys were melted in the vacuum induction furnace. The crucible used was ZrO_2. The as-cast alloys were submitted to a heat treatment in order to homogenize and stabilize the gamma phase at room temperature. The samples were heated for 5 hours at 1000°C. following by water quenching. Hot rolling was performed at 650 °C in three height steps: 50, 65 and 80% of their initial thickness. During the hot rolling, homogenized alloys were encapsulating in copper sheets to avoid oxidation and pyrophoric reactions.

Samples were generally cut by metallographic cutters using SiC abrasive discs. The samples were grinded with 1200 mesh SiC paper. After grinding, the samples were polished using a 9 μm, 3 μm and 1 μm diamond suspension. Electrolytic etching was performed with a solution of 6 parts of a 10% H_2CrO_4 solution and 1 part of 10% HNO_3. The voltage was 2 V for approximately 20 s.

Chemical composition was obtained by Induced Coupled Plasma Optical Emission Spectroscopy (ICPOES) (brand: Spectro – model: Spectroflame) except carbon that were determined by combustion method (brand: Eltra - model: CS-2000). To obtain reliable chemical composition results, the chemical analysis was performed in 6 g of material collected in several parts of the as-cast samples. The chemical composition results were presented from an average of 3 analyses. The optical and electronic microscopies were employed in the as-cast and homogenized samples. It was used Carl Zeiss Axioimager A1m optical microscope and FEI Quanta FEG 250 Scanning Electron Microscope (SEM).

The crystalline phase and texture will be evaluated by x-ray diffractometry with Cu kα radiation. Both analyses were performed with a Panalytical diffractometer model Empyrean. (110), (200), (211) and (310) pole figures were obtained and then the orientation distribution function (ODF) were calculated by MTEX software [12].

3. RESULTS

The table 1 shows chemical composition U-Mo alloys. It was observed that the crucible did not contaminate the alloys. The as-cast diffractograms (Fig. 1) show that the alloys stabilized the γ-phase. The U9.5Mo x-ray diffraction peaks are dislocated to the right in comparison with U7.4Mo, this is due the fact that de Mo atom is smaller than U atom and a decrease in lattice parameter occurs as the content of Mo is increased.

Table 1: Chemical composition of U-Mo alloys ($mg.kg^{-1}$ ± standard deviation). Values without standard deviation are below the detection limit of the equipment.

Element	U7.4Mo	U9.5Mo
N	9.75 ± 0.49	12.2 ± 2.5
C	260 ± 20	420 ± 20
Al	1335 ± 31	1000 ±42
B	43.1 ± 3.6	12.54 ± 0.01
Cr	< 1.00	< 1.27
Cd	< 2.08	< 2.64
Mn	253.2 ± 4.3	263.9 ±1.5
Fe	390.8 ± 17.8	393.0 ± 5.4
Co	< 0.028	< 0.028
Cu	5.85 ± 0.01	< 1.08
Zn	11.03 ± 0.98	15.9 ± 1.1
Ag	< 0.99	< 1.26
Zr	< 0.36	< 0.46
Ni	62.70 ± 0.01	77.4 ± 2.2
Gd	< 1.49	< 1.90
Si	< 0.008	< 0.008
V	< 0.006	< 0.006
Nb	< 0.002	< 0.002
Mo	73833 ± 80	95350 ± 650
W	< 0.041	< 0.041

Fig. 2 shows the as-cast U9.5Mo and U7.4Mo micrographs obtained by optical microscopy. Equiaxed grains with dendritic structure originated from solidification in the induction furnace were observed. The U7.4Mo alloy has a coarser dendritic structure than the U9.5Mo alloy.

Molybdenum has higher corrosion resistance than the U and, as a consequence, the metallographic etching is more severe in regions with lower Mo content concluding that the alloys solidification starts in regions with higher molybdenum concentration and microsegregation are presented in as-cast UMo alloys. This behavior is justified because the addition of molybdenum increases the melting point and therefore the regions with the highest molybdenum concentration solidify first [13]. Grains average sizes are 152.5 ± 28.8 μm and 76.1 ± 5.5 μm for the U7.4Mo and U9.5Mo as-cast alloys, respectively.

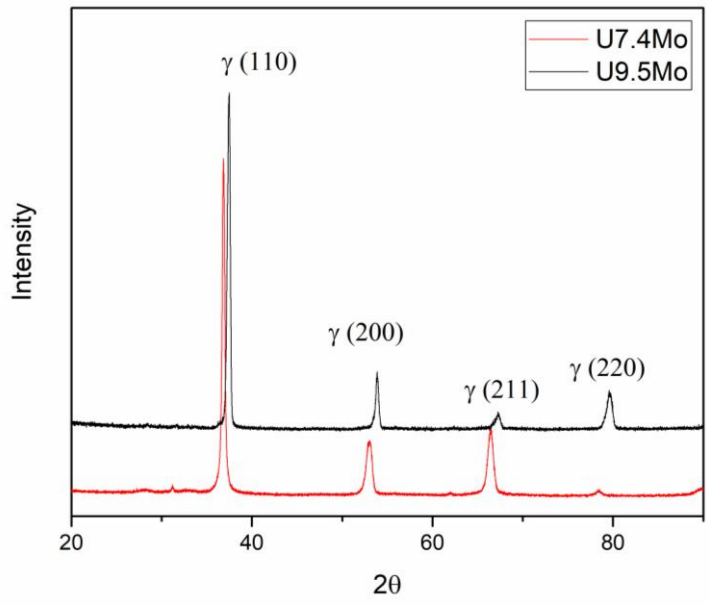

Figure 1: As-cast U7.4Mo U9.5Mo diffractograms.

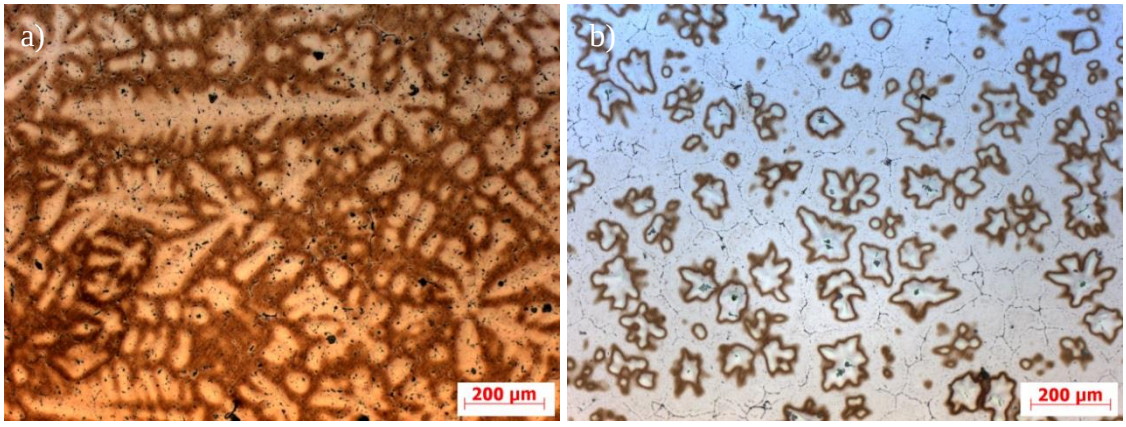

Figure 2: Micrographs of the as-cast U7.4Mo (a) and U9.5Mo (b).

The contrast differences in backscattered electrons (BSE) images obtained by scanning electron microscope (Fig. 3) confirm the microsegregation of the as-cast alloys. It is noticed in the center of the dendritic grain darker contrast due to higher concentration of Mo. In micrographs by electron microscopy, it is also possible to observe the coarse dendritic structure of the U7.4Mo alloy.

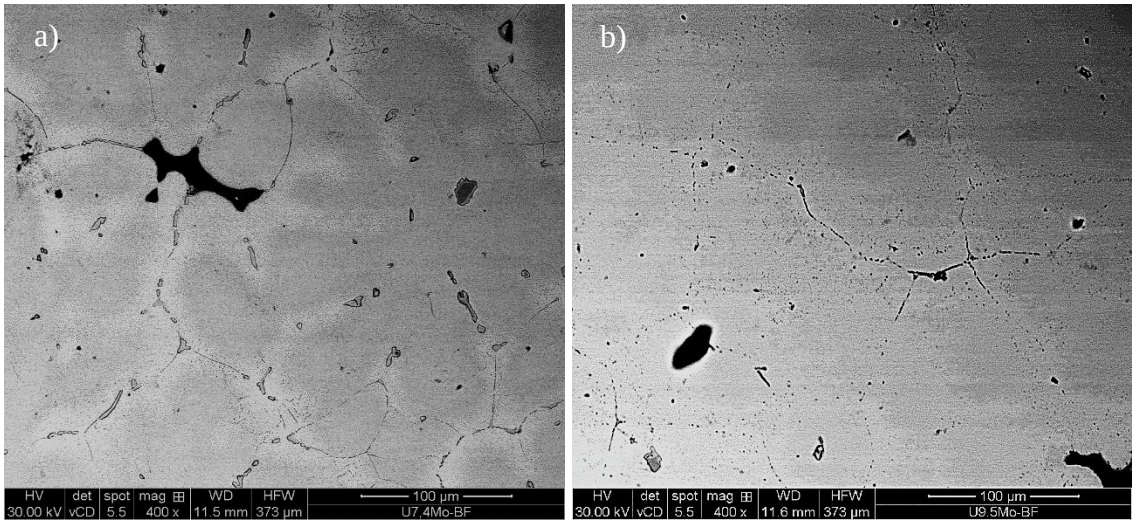

Figure 3: Micrographs obtained by backscattered electrons from the as-cast U7.4Mo (a) and U9.5Mo (b).

The results of the as-cast U-Mo alloys indicate the necessity for homogenization of the alloy. Microstructure region with low Mo content is more favorable for decomposition the γ-U from the eutectoid reaction UMo = U_2Mo + α-U [14] making an important factor for the production of monolithic nuclear fuels. Homogenized UMo alloys are necessary to obtain for decreasing phase transitions probability during the irradiation of these alloys [14].

Considering that the as-cast alloys U7.4Mo and U9.5Mo showed microsegregation, a homogenization treatment was performed. As in the as-cast samples, the gamma phase was found homogenization treatment. These results are seen in the x-ray diffractograms (Fig. 4).

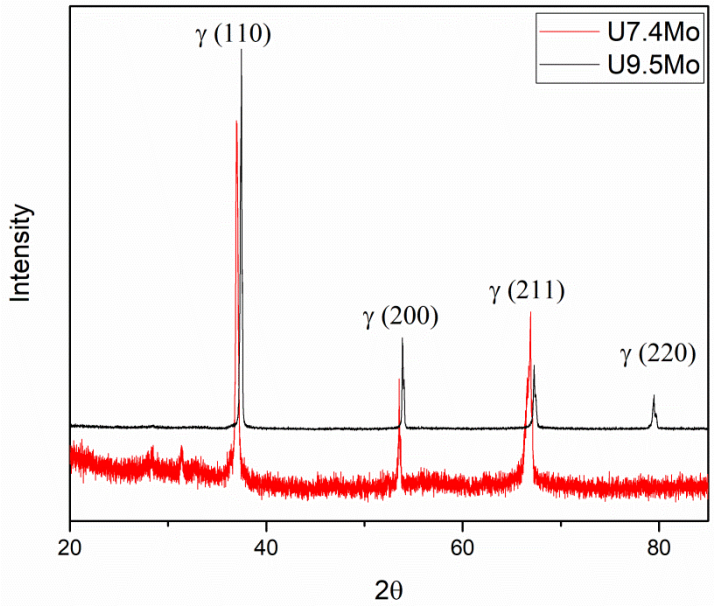

Figure 4: Diffractograms of the U7.4Mo U9.5Mo thermally treated alloy.

Another aspect observed in the diffractogram of the thermally treated U-Mo alloys is the width of the peak which is reduced as the temperature increases indicating refinement of the alloy. The microstructures of the thermally treated alloys are shown in Fig. 5. As observed in these figures the dendrites in both alloys are consumed.

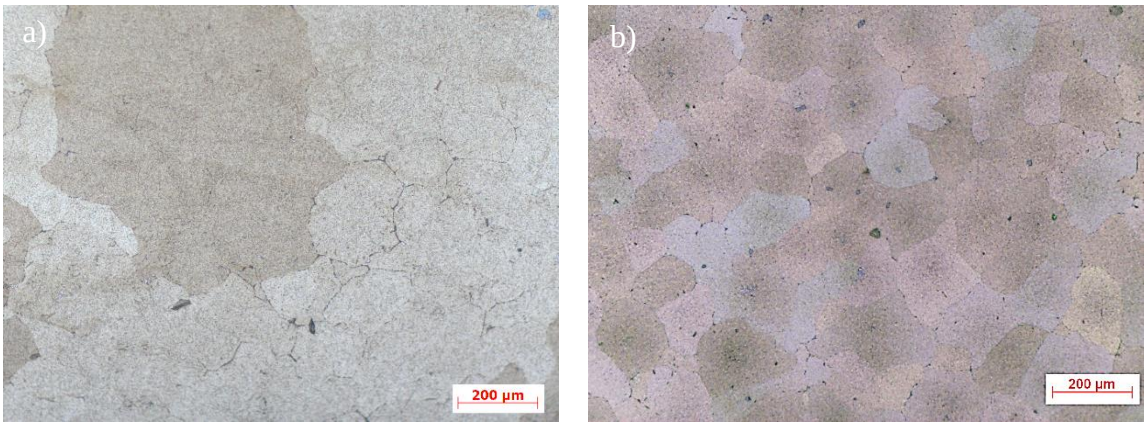

Figure 5: Micrographs of the heat treated U7.4Mo (a) U9.5Mo (b).

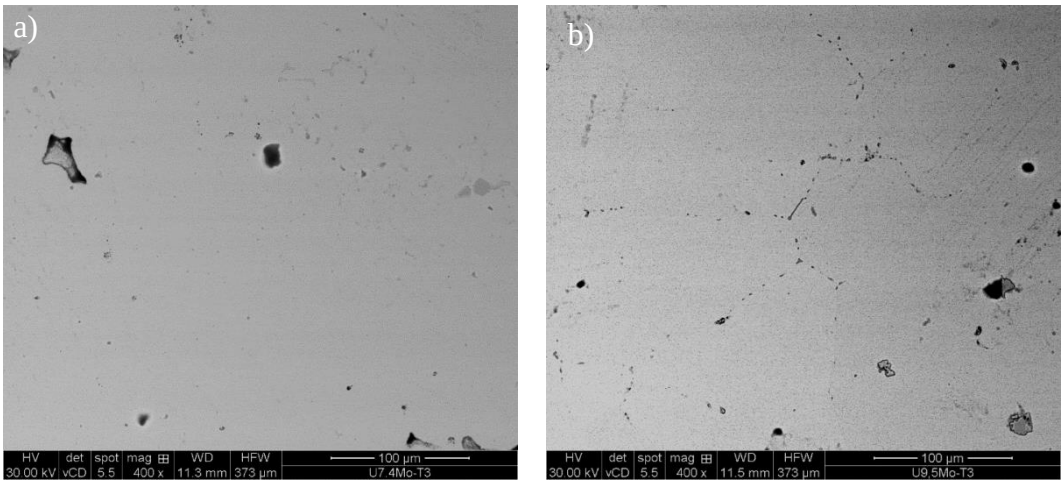

Figure 6: Heat treated U7.4Mo (a) U9.5Mo (b) Electron backscattered micrographs.

BSE images (Fig. 6) show that the homogenization is obtained. The homogenization treatment diffuses the Mo in the alloy. It can be observed in Fig. 5 equiaxied grains and the average grain size obtained was 174.5 ± 27.6 µm for U7.4Mo and 97.5 ± 4.5 µm for U9.5Mo. Comparing the mean grain size of as-cast samples with the homogenized alloys a growth of 14.4% for U7.4Mo and 28.1% for U9.5Mo. The largest increase in grain size for the U9.5Mo alloy can be attributed to carbon concentration. Clarke et al. reported that the grain growth could be influenced by carbon content [14]. The grain size of the homogenized samples did not change significantly the grain size of the as-cast alloy.

Fig. 7 shows the texture results for U7.4Mo and U9.5Mo alloys deformed in 50%, 65% and 80%. In general, it is noted that the gamma fiber is present in all deformations, however this fiber is more prominent up to 65% deformation. The intensity of the γ fiber decreases with

increasing deformation. The alpha and theta fibers are increased by 80% for both alloys. Similar results were observed for the cold rolled UZrNb alloy [13]. In body centered cubic materials it is common to observe the intensification of the alpha fiber as a mechanism of deformation around the dense crystalline plane (111). The textures (001)[101] may be related to the recovery of the material during heating in the hot rolling process.

The alpha, theta fiber textures rinsing in 80% deformed alloys contributes to the isotropic properties of the material, generating a great interest in nuclear applications, resulting in symmetrical swelling behavior [13].

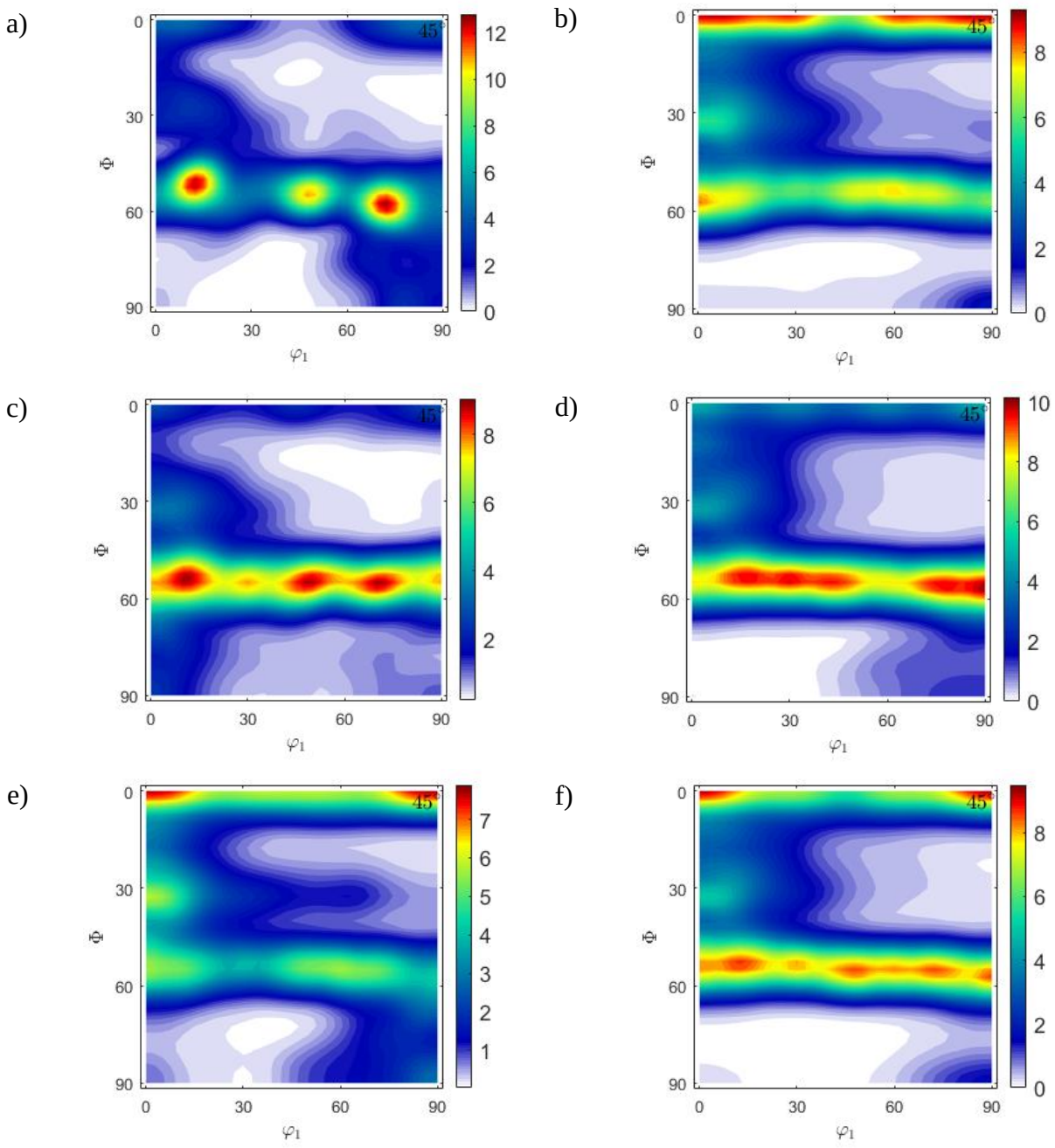

Figure 7: ODF φ_2 = 45° section for the U7.4Mo deformed at 50 (a), 65 (c) and 80 (e)%; U9.5Mo deformed at 50 (b), 65 (d) and 80 (f)%.

4. CONCLUSIONS

The microstructure, texture results of homogenized and deformed U7.4Mo and U9.5Mo give the following conclusions:

1. The as-cast alloys were generation of coarse dendritic structures, microsegregation and have a gamma phase.
2. The homogenization treatment consumed the dendrites and eliminated the microsegregation without significant grain growth.
3. The deformed uranium molybdenum alloys presented strong γ fiber texture (111) <uvw> and moderated α-fiber texture (hkl) <110>.
4. It was noted the evolution of alpha fiber as the increasing deformation contributing to the reduction gamma fiber reducing anisotropic properties of the material.

REFERENCES

1. E. E. Pasqualini, A. B. Robinson, D. L. Porter, D. M. Wachs, M. R. Finlay, "Fabrication and testing of U7Mo monolithic plate fuel with Zircaloy," *Journal of Nuclear Materials*, **Vol. 479**, pp. 402–410 (2016).
2. D. M. Wachs, "RERTR Fuel Development and Qualification Plan", https://inldigitallibrary.inl.gov/sites/sti/sti/3610331.pdf (2007).
3. V. P. Sinha, G.J. Prasad, P.V. Hegde, R. Keswani, C.B. Basak, S. Pal, G.P. Mishra, "Development , preparation and characterization of uranium molybdenum alloys for dispersion fuel application," *Journal ofAlloys and Compounds*, **Vol. 473**, pp. 238–244 (2009).
4. F. B. Vaz de Oliveira. *Desenvolvimento de um combustível de alta densidade à base da liga urânio-molibdênio com alta compatibilidade em altas temperaturas*, Instituto de Pesquisas Energéticas e Nucleares, São Paulo & Brazil (2008).
5. V. P. Sinha, P. V. Hegde, G. J. Prasad, G. K. Dey, H. S. Kamath, "Phase transformation of metastable cubic γ-phase in U-Mo alloys," *Journal ofAlloys and Compounds*, **Vol. 506**, pp. 253–262 (2010).
6. D. A. Lopes. *Interação entre precipitação e recristalização em liga de urânio contendo nióbio e zircônio (Mulberry alloy)*, Universidade de São Paulo, São Paulo & Brazil (2014).
7. G. K. Suryaman, M. W. Wildan, Supardjo, Y. D. A. Susanto, "Production of uranium−molybdenum alloy as a candidate for nuclear research reactor fuel," *Urania*, **Vol. 24**, pp. 135–142 (2018).
8. H. P. Jaime Lisboa, J. Marin, M, Barrera, "Engineering of fuel plates on uranium-molybdenum monolithic: critical issues," *World Journal of Nuclear Science and Technology*, **Vol. 5**, pp. 274–286 (2015).
9. C. T. Woolum. *Fabrication and characterization of uranium- molybdenum-zirconium alloys*, Texas A&M University, College Station & United States of America (2014).
10. E. Perez, B. Yao, D. D. Keiser, Y. H. Sohn, "Microstructural analysis of as-processed U-10 wt.%Mo monolithic fuel plate in AA6061 matrix with Zr diffusion barrier," *Journal of Nuclear Materials*, **Vol. 402**, pp. 8–14 (2010).
11. C. R. Clark, G. C. Knighton, M. K. Meyer, G. L. Hofman, "Monolithic fuel plate development at Argonne National Laboratory," *International Meeting on Reduced Enrichment for Research and Test Reactors*, Chicago, October 5-10 (2003).

12. R. Hielscher, H. Schaeben, “A novel pole figure inversion method : specification of the MTEX algorithm,” *Journal of Applied Crystallography*, **Vol. 41**, pp. 1024–1037 (2008).
13. D. A. Lopes, T. A. G. Restivo, N. B. De Lima, A. F. Padilha, “Gamma-phase homogenization and texture in U-7.5Nb-2.5Zr (Mulberry) alloy,” *Journal of Nuclear Materials*, **Vol. 449**, pp. 23–30 (2014).
14. A. J. Clarke et al., “Microstructural evolution of a uranium-10 wt.% molybdenum alloy for nuclear reactor fuels,” *Journal of Nuclear Materials*, **Vol. 465**, pp. 784–792 (2015).